

Nonlinear local contourlet energy pattern for image retrieval applications

T. G. Subash Kumar ^{1*}, V. Nagarajan ²

¹ Faculty of Electrical and Electronics, Department of ECE, Sathyabama institute of science and technology, Chennai, 600119, India

² Adhiparasakthi Engineering College, Melmaruvathur, 603319, India

*Corresponding author E-mail: gtsubash@gmail.com

Abstract

Local patterns are effective in different machine vision problems such as pedestrian identification, lane categorization, face recognition, retrieving required image etc., Various local patterns are introduced by the researchers in order improve the efficiency, however these local pattern operates on a fixed pixels that are predetermined and are same for all the images. The features thus extracted from these predetermined pixels are limited. In this paper a novel technique called nonlinear local contourlet energy pattern (NLCEP) is introduced which extracts the local pattern from the pixels that are selected dynamically in run time which will vary with the images. Also to improve the feature robustness the features are extracted in Contourlet domain instead of the spatial domain. With this approach the dominant image features like lines/curves are better represented by the NLCEP and its features are effectively used in image retrieval system. The performance of this method is validated by doing different experiments with the standard available databases (viz Corel 1K, Corel 10K and Brodatz). The test results with different experiments shows that the proposed approach provides better performance for image retrieval applications.

Keywords: Local Pattern; Nonlinear Local Contourlet Energy Pattern; Local Tetra Pattern; Content Based Image Retrieval.

1. Introduction

CBIR, retrieval of images based on its content is the right solution for the image retrieval problem and is used in different areas image processing application. Some of them are: e-commerce for getting the required commodities, satellite imaging for analyzing the required images, grouping the images based on person's identity and so on. In contrast to other image retrieval techniques, CBIR works on the features that are extracted from visual objects to retrieve the image of interest. The visual objects are represented as descriptor such as contours, shape, texture, binary patterns etc. The effectiveness of the image retrieval depends on the amount of unique information captured by the features from an image. In general spatial domain and transform domain techniques are the two different feature extraction techniques used in image retrieval applications. Spatial technique uses the image intensity values to extract the descriptors and the transform domain technique use the transform coefficients to extract the descriptors.

The features that are extracted in spatial domain are most commonly used in time critical applications due to its simplicity, but it is less accurate and easily affected by the disturbances like lighting and noise. Some features that uses image gray scale values directly are local binary pattern [1], [2], gray level Co-occurrence [3], image gradient [4] and so on. However the performance of the transform domain features are much better compared to spatial features but at the cost of complexity. With very high powerful CPU processors in the market, researchers are focussing now more on the performance rather than the system complexity. The image features are extracted from different image transforms like Fourier [5], DCT [6], Wavelet [7], Ridgelet [8], contourlet [9], shearlet [10], [11] and so on. The major factor that decides the efficiency

of transform domain features is the representation of image lines and curves by image transform and also the performance of the features that are derived from it. Statistical features generally include the overall image variations into the feature vectors [12], [13]. Good amount of work in going on recently for using the local transformed coefficients such as wavelet based LWP [14], energy based on Shearlet bands [15], local patterns based on DCT [16] etc.

Recently local patterns are used by different researchers and are successful in many machine vision problems such as CBIR [17], facial identification [18], fingerprint detection [19], texture identification [20], classification of person into female and male [21], analysis of paralysis on face [22], examination of medical images [23], finding the malformation in mammogram images [24] etc. Lot of works were done to increase the efficiency of LBP in the spatial domain such as ternary pattern (LTP) [25], Completed LBPs [26], Dominant LBPs [27], Local Quantised Extrema Quinary Pattern (LQEQRyP) [28] and so on. To improve the robustness, transformed coefficients are used to extract local features rather than image intensity values.

1.1. Related works

Timo Ahonen et al introduced the local Fourier based histogram [29] in which the local pattern is derived after transforming image using the discrete Fourier transform to make the feature vector rotation invariant. Shiv Ram et al, extracted the local pattern in wavelet domain by using the correlation of local neighbours with the center pixel and are used for retrieving the computer tomography (CT) medical images. Maryam et al., [30] used LBP with stationary wavelet transform Directional to identify the human action. Lijian Zhou et al [31] combine the curvelet transform features with LBP using the method of local property preservation and used this feature for face recognition to improve the perfor-

mance of the system. To make face recognition as expression invariant Hemprasad et al [32] fused the LBP features with the features extracted from contourlet coefficients to produce more robust feature vector. Jiangping et al extracts the local features from Shearlet coefficients [33] for the design of rotation insensitive classification system by decomposing the image using shearlets and constructing the local features using the shearlet coefficients which is again encoded to make them insensitive to rotation.

Most of these local feature extraction methods depend on the directions or gradients derived/calculated from set of image pixels over the neighborhood and the location of the pixels are static or same for all the images. Here, a modified nonlinear local approach based on contourlet transform is introduced for CBIR where local contourlet features are extracted from the contourlet coefficients that are dynamically picked and will vary with the images. The contourlet coefficients are selected that gives smoothness over the contours of the local region and the features are derived using these coefficients. This method represents the contour smoothness and curves more accurately that are one of the important image characteristics. This new method is evaluated by using the standard databases and the experimental results show the improvement in retrieval performance when compared with the existing techniques.

Following sessions are organized as follows; Section 2 discusses the motivation and modeling of the proposed nonlinear local contourlet energy pattern. The CBIR system based on the new local contourlet features is given in Section 3 and the performance evaluation of the proposed technique is presented in section 4.

2. Nonlinear local contourlet energy pattern

2.1. Motivation

Despite the fact that the existing local patterns are attractive, it has its own limitations

- 1) It fails to capture the global image variations
- 2) Spatial features are always more prone to external noise
- 3) The information captured by the feature vectors is limited as local patterns work on the predefined set of pixels

To overcome these limitations, nonlinear contourlet local pattern is proposed that uses contourlet transform to develop a nonlinear local binary pattern. Contourlet transform is used in this approach to capture more global information and also less prone to external disturbances. Also, since the local pattern is formed in a non-uniform way, it will have more image features compared to the other conventional local pattern techniques.

2.2. Modelling

The main goal of the non-linear local contourlet energy pattern is to identify and catch the local nonlinear image structures such as contours to improve the feature efficiency. Assume that the pixel under consideration is on the contourlet curve, then the contour smoothness can be extracted by navigating over its smoothness and the path of the navigation will be determined by the neighbouring contourlet coefficients. Let I the image under consideration and $I(i,j)$ be the image pixel that are used to derive the local pattern, then the direction of the path can be determined by navigating over the direction with least contourlet energy variance in all possible directions as shown in Fig 1. The bold line shows the navigation path with least contourlet energy variance when over its neighbours.

For the input image I , let C_d^i be the contourlet transformed sub-image at direction d and scale i . Assume the point of interest on the navigation path for extracting the pattern in contourlet domain is $C_d^i(x,y)$ the direction of path can be found by navigating towards the point with least contourlet energy difference.

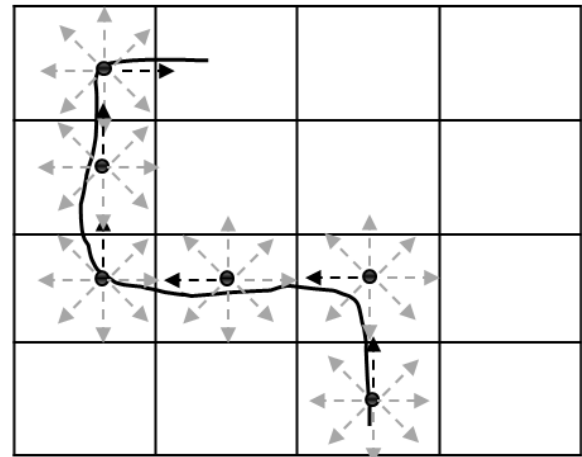


Fig. 1: Traversing over the curve.

The contourlet energy at a point in the given scale is calculated as shown in Fig 2 and is given by

$$\text{Energy } E_i(x,y) = \sqrt{\sum_{p=1}^d |C_p^i(x,y)|^2} \tag{1}$$

Where $E_i(x,y)$ is the contourlet energy at (x,y) of scale i .

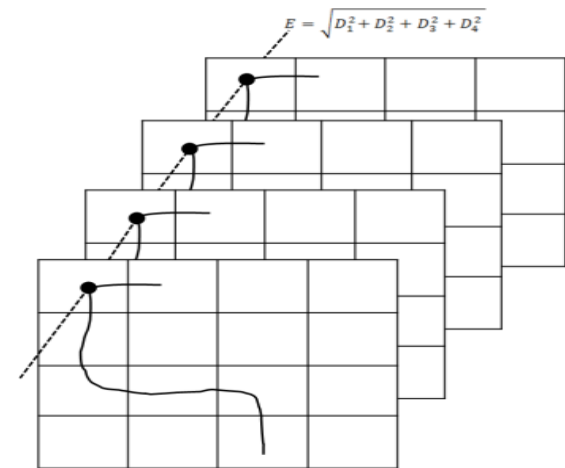


Fig. 2: Energy at a Contourlet Point.

In contrast to the other local technique, the center pixel for estimating the curve direction by NLCEP is picked dynamically for each symbol and an eight symbol pattern is derived for each point in the curve as in the Fig 1. For a point (x_c, y_c) on the curve the non-linear contourlet pattern is defined as

$$\text{NLCEP}(x_c, y_c) = \sum_{k=0}^{L-1} \text{DR}(C_k) S^k \tag{2}$$

where L is the curve length that is used to derive the NLCEP pattern, S is the number of unique symbols in NLCEP, C_k is the center pixel used for deriving the k^{th} symbol and $\text{DR}(k)$ is the unique number that are assigned to each directions on the navigation path. The center pixel C_k will vary for each symbol and the next center pixel is chosen as given below.

$$C_{k+1} = C_k |_{\{\min(\text{abs}(E_k - E_n))\}}, \quad n=0 \text{ to } N-1 \tag{3}$$

Where, E_k is the contourlet energy of k^{th} pixel, E_n is the contourlet energy of the neighbouring pixels and N is the total number of neighbours. The direction number $\text{DR}(p)$ is formed by considering all the possible directions that the path can navigate. Here since the pixels over 3×3 neighbours are considered there will be eight different directions the path can navigate and is given by the eqn (4)

$$\text{DN}(p) = n ; \min \text{ of } (E_p - E_n) \text{ for } n = 0 \text{ to } N - 1 \tag{4}$$

With length of curve as eight and eight unique symbols for each point there will be $8^8 = 16777216$ unique bins in the local pattern. To handle this large number of bins, the eight directions are divided into two four directions as in Fig. 3 so that there will be $4^8 = 65536$ bins in each four directions and the total of 131072 bins in the local pattern.

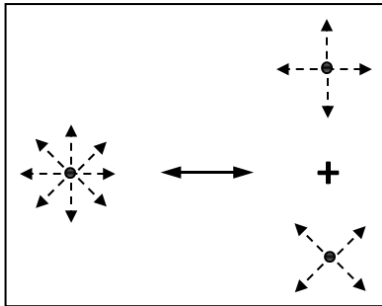


Fig. 3: Eight Directions into Two Four Directions.

To reduce the bins further local tetra pattern [34] is used to represent directions. Consider that there are four unique symbols (1 to 4) for a pixel of interest (x_c, y_c) , then the nonlinear local contourlet pattern is defined as

$$NLCEP^k(x_c, y_c) = \sum_{l=0}^{L/2-1} DR(C_l)S^l \quad (5)$$

Here k represents the number of four-directions and can be either zero or one. With this the input image is split into two tetra patterns and the equivalent binary representation can be formed using [33] so that there will be $12 \times 256 \times 2 = 6144$ features. The features can be reduced by using the uniform patterns proposed in [35]. With this approach the number of patterns can be reduced by considering only the uniform symbols. Uniform symbols are the one with minimum transition between ones and zeros and the transition should be less than or equal to two. Hence for 3×3 neighbours the number of bins can be reduced from 256 to 58 and adding one bin for non-uniform symbols making the bins count to 59. With this method the number of bins in nonlinear local contourlet energy pattern is reduced to $12 \times 59 \times 2 = 1416$ features.

Histogram is one of the effective features that can be derived from the nonlinear local contourlet energy pattern. Assume $NLCEP^i(i, j)$ be the nonlinear local contourlet energy pattern, then the histogram feature is given by

$$NHist^i(k) = \sum_{i=0}^{M-1} \sum_{j=0}^{N-1} \delta(NLCEP^i(i, j) - k) \quad (6)$$

Here M and N are the image size, $k = 1$ to 59 and $\delta(k)$ is given by

$$\delta(k) = \begin{cases} 1 & ; k = 0 \\ 0 & ; k \neq 0 \end{cases} \quad (7)$$

The output of the contourlet feature system will be 12 pairs of histogram with each of size 59 bins as shown in Fig 4.

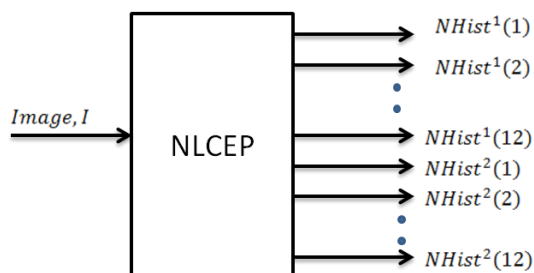


Fig. 4: Input and Output of NLCEP Feature System.

2.3. Advantages of NLCEP

The positive side of NLCEP over the similar techniques are.

- 1) Conventional methods extract the local patterns from the constant pixel locations which do not vary with images that capture only the local image discontinuities whereas it fails to capture the global image features. In contrast NLCEP derive the pattern using the pixels that are selected in runtime which helps to represent the image features more effectively. Also the contour smoothness can be more precisely represented by contourlet transform that helps NLCEP to boost its performance.
- 2) Conventional local pattern techniques capture the local features using the gradients that are derived directly from the image intensity values can be easily disturbed by the external noise. Also, it considers only the gradient across the edges not the smoothness over the edges. Contourlet directions overcome these two limitations: it is less disturbed by external noise and also it captures the smoothness over the edges or contours. This makes NLCEP features better for image retrieval applications.

3. NCLEP based CBIR system

Feature extraction of CBIR system will happen both in training and classification/retrieval. In training phase, the NLCEP features are derived from the images available in the database and are stored with proper indexing. The number of features extracted from an image plays a key role in the size and complexity of the database; hence it is required to keep the minimum number of features for better design of the image retrieval system. In retrieval stage, the query image will be given input to the system and the NLCEP features are extracted from the query image. The images whose NLCEP feature matches closely with the query image will be retrieved and will be given as output from the CBIR system. Fig. 5 shows NLCEP based CBIR system. Following are the steps that are used by this system.

- 1) Feed the query image; convert to single plane if the input is colour with three planes.
- 2) Perform contourlet decomposition on the query image
- 3) Estimate the contourlet energy from different directions as in eqn. (1)
- 4) Form the two four directional nonlinear contourlet pattern
- 5) Apply the feature optimization technique
- 6) Calculate the image histogram of the nonlinear contourlet pattern
- 7) Combine the NLCEP from different directions.
- 8) Measure the distance of NLCEP features of query image with the database images.
- 9) Get the best M nearest image from the database which is close to the query image.

Assume the size of the NLCEP features be B , R be the NLCEP feature of the input query image and T_i be the NLCEP features of the images that are in database, where i is the image index in database. To retrieve the top M best image from the database that is close to the query image chi square distance [36] is used as in eqn. (8),

$$\chi_i^2(R, T) = \sum_{b=1}^B \frac{(R_b - T_{ib})^2}{R_b + T_{ib}} \quad (8)$$

Chi square distance helps to compare the two histograms effectively and also helps to retrieve the top M best images from the database.

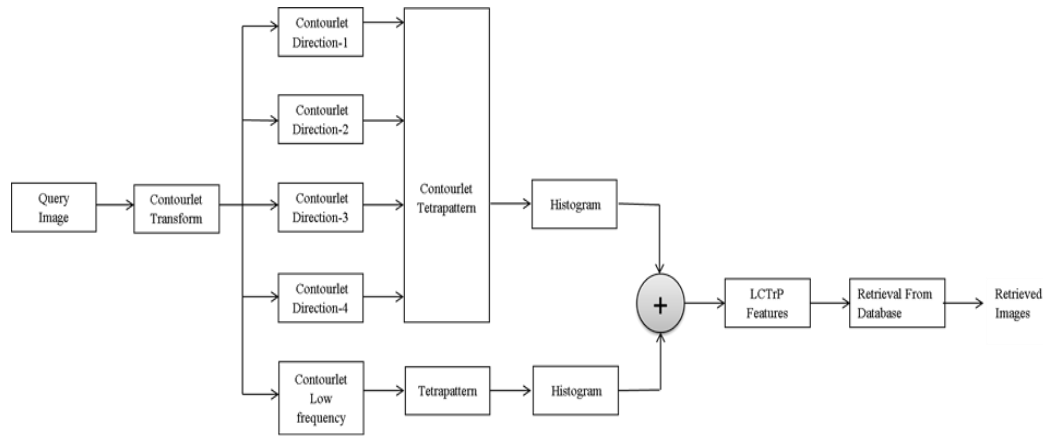


Fig. 5: NLCEP Based CBIR System.

4. Performance evaluation

Three standard image databases that are freely available are used in this work to measure the performance of the proposed method. The databases are 1000 images from Corel-1K [37], 10,000 images from Corel-10K [38] and 112 texture images from Brodatz [39]. The images from databases are grouped into multiple categories and are used for different tests. For test-1, database is created using the datasets in [37] that contain thousand pictures and are grouped into different categories based on their characteristics. The images in Corel1K database is already arranged in sequential order so that each 100 images belong to a certain category. For Test-2, database is created using the images from datasets in [38] that contain ten thousand pictures and are already grouped into different categories. For Test 3, images are used from the datasets in [39] that contain 112 texture classes. The images are sub divided into 128 x 128 and 256 x 256 half overlapped areas so that the total of 6608 (59 x 112) images in the database. The consolidated details of the test datasets used for the experiment are listed in the Table-1.

Table 1: Datasets for Test

Sl No	DATASET	Category	No. of image per category	Image per database
1	Corel1K	10	100	1000
2	Corel10K	80	Differ	10000
3	Brodatz	112	59	6608

Three different tests were done on various datasets and best matched M images are retrieved from the datasets and five different tests we done with M = 10 to 50 in steps of 10. The NLCEP features are derived from the input query image and are matched with the NLCEP features in the database using the chi square distance as in eqn (8). The performance of NLCEP is validated using Average Retrieval Precision (ARP) and Average Retrieval Rate (ARR) and is given as in eqn (9).

$$ARP = \frac{\text{Precision}}{N} \quad \& \quad ARR = \frac{\text{Recall}}{N}$$

$$\text{Precision} = \frac{\#SR}{\#TR} \quad \& \quad \text{Recall} = \frac{\#SR}{\#NQ} \tag{9}$$

Where N is the total number of retrieval happened, #SR number of successful retrieval, #TR Target output images and #NQ number of query class images. To compare the retrieval results of NLCEP Local Tetra Pattern [34], Bag of filters [40] and Wavelet pattern [41] were used.

4.1. Experiment-1: corel 1k database (natural images)

Table 2: Retrieval Performance (ARP) with Dataset-1

Techniques	Target output images (N)				
	10	20	30	40	50
NLCEP	80.8	75.1	71.2	66.8	60.5
BOF-LBP	72.8	69.3	63.9	58.5	55.3
DBWP	69.8	64.2	60.2	57.6	53.2
LTrP	66.5	62	57.3	54.7	50.2

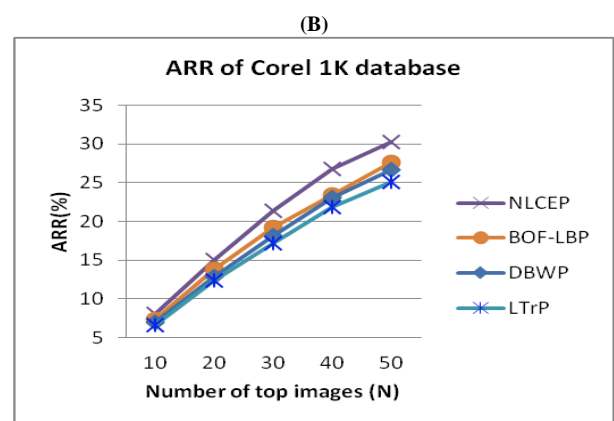
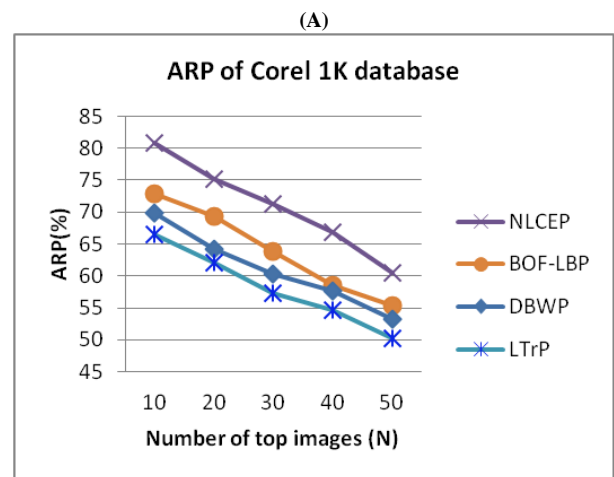


Fig. 6: Retrieval Efficiency for Dataset – 1 (A) ARP (%) and (B) ARR (%)

First experiment uses the datasets from Corel 1K that contain images from ten different classes. The retrieval performance with dataset-1 is listed in Table – 2 for different target output images. Here five different tests are done with different target output images ranging from ten to fifty in steps of ten. From the table it is quite clear that the performance with NLCEP is better than other equivalent methods. The average increase in ARP for NLCEP is 12.74%, 9.86% and 6.9% respectively when compared with LTrP, DBWP and BOF-LBP. Fig. 6 (a) and (b) gives the retrieval effi-

ciency using ARP and ARR respectively for different target output images.

4.2. Experiment-2: corel 10k database (natural images)

Experiment-2 uses the datasets from Corel 10K that contain images from eighty different classes. The retrieval performance with dataset-2 is listed in Table – 3 for different target output images. The average increase in ARP for NLCEP is 5.9%, 5.2% and 3.5% respectively when compared with LTrP, DBWP and BOF-LBP. Fig. 7 (a) and (b) gives the retrieval efficiency of dataset-2 using ARP and ARR respectively for different target output images.

Table 3: Retrieval Performance (ARP) with Dataset-2

TECHNIQUES	TARGET OUTPUT IMAGES (N)				
	10	20	30	40	50
NLCEP	43.1	36.4	31.3	27.8	26.1
BOF-LBP	39.2	33.8	27.5	24.2	22.6
DBWP	37.1	33.1	25.6	22.6	20.1
LTrP	36.3	32.7	25.1	21.4	19.5

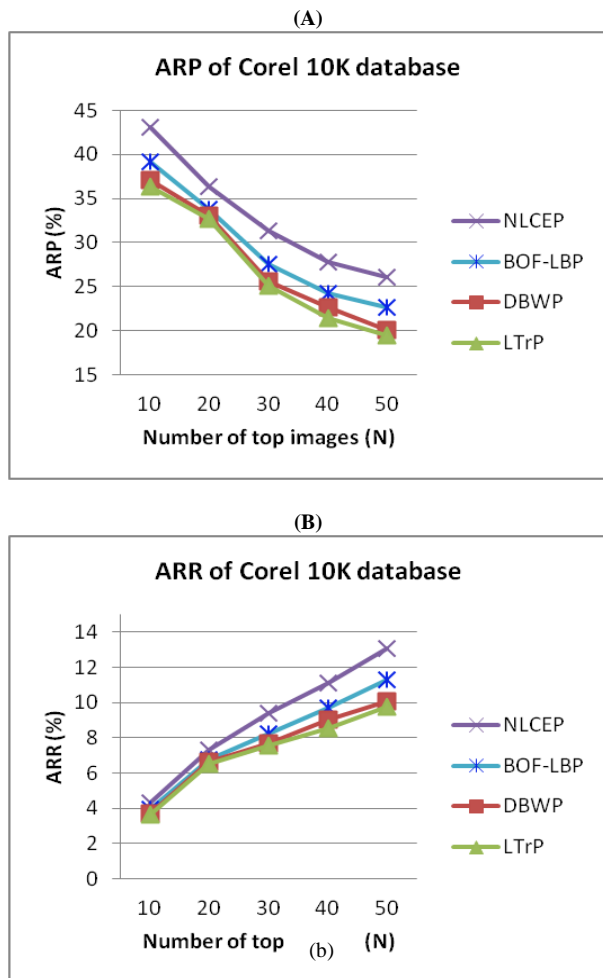


Fig 7: Retrieval Efficiency for Dataset – 2 (A) ARP (%) and (B) ARR (%).

4.3. Experiment-3: brodatz DB (texture images)

Experiment-3 uses the datasets from Brodatz that contain images from 112 different classes. The retrieval performance with dataset-3 is listed in Table – 4 for different target output images. The average increase in ARP for NLCEP is 5.5%, 4.1% and 2.8% respectively when compared with LTrP, DBWP and BOF-LBP. Fig. 8 (a) and (b) gives the retrieval efficiency of dataset-3 using ARP and ARR respectively for different target output images

Table 4: Retrieval Performance (ARP) with Dataset-3

Techniques	Target Output Images (N)				
	10	20	30	40	50
NLCEP	96.5	94.2	92.3	88.6	87.1
BOF-LBP	94.1	92.1	88.9	85.6	83.8
DBWP	93.4	91.5	86.2	84.3	82.6
LTrP	92.2	89.8	85.3	82.4	81.3

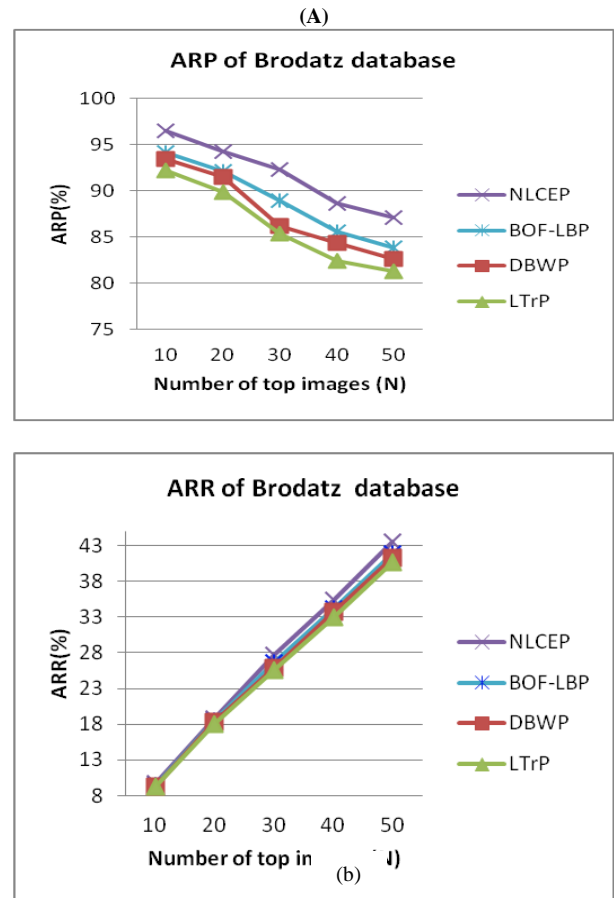


Fig. 8: Retrieval Efficiency for Dataset – 3 (A) ARP (%) and (B) ARR (%).

The increase in the efficiency of image retrieval rate using NLCEP can be justified with the following points

- 1) Existing methods represent the local image features using only the neighbouring pixels but the NLCEP capture the image features beyond the local region that helps NLCEP to capture more effective information.
- 2) NLCEP uses the energy from transform domain coefficients that is less disturbed by noise.
- 3) Since NLCEP derive the features from the pixels whose location varies with images based on its characteristics, it can effectively capture the local contour and its smoothness information than other methods

5. Conclusion

In this paper a new method called Nonlinear Local Contourlet Energy Pattern (NLCEP) is proposed for CBIR applications. To increase the retrieval efficiency, NLCEP extracts the features from the energy of contourlet coefficients that varies with images based on its characteristics in runtime. The efficiency of the proposed method is evaluated using the standard databases and the results show that NLCEP features are best suited for CBIR applications than similar methods. The current work is limited to gray scale images and this work can be extended to the colour images by combining NLCEP with a suitable colour feature. Also in this work, the length of the pattern is considered as eight and analysis can be made by increasing the pattern length.

Acknowledgement

The authors are very much thankful to the editor and anonymous reviewers for their valuable comments, suggestions and other directions to improve the quality of this manuscript. Also, authors thank the management of Sathyabama institute of science and technology and Adhiparasakthi engineering college for their constant support and motivation.

References

- [1] Li Liua, et al (2012), extended local binary patterns for texture classification, Vol 30, *Image and Vision Computing*, pp 86–99. <https://doi.org/10.1016/j.imavis.2012.01.001>.
- [2] MH Shakoor and Reza Boostani (2017), Extended Mapping Local Binary Pattern Operator for Texture Classification, Vol 31, *International Journal of Pattern Recognition and Artificial Intelligence*.
- [3] Yang Hongbo, Hou Xia (2014), Histogram modification using grey-level co-occurrence matrix for image contrast enhancement, Vol: 8, *IET Image Processing*, pp. 782 – 793.
- [4] T.N. Tan, K.D. Baker (2000), efficient image gradient based vehicle localization, Vol: 9, *IEEE Transactions on Image Processing*, pp. 1343 – 1356. <https://doi.org/10.1109/83.855430>.
- [5] I.S. Uzun, A. Amira, A. Bouridane (2005), FPGA implementations of fast Fourier transforms for real-time signal and image processing, Vol: 152, *IEE Proceedings - Vision, Image and Signal Processing*, pp. 283 – 296.
- [6] Y. Asnath Victy Phamila, R. Amutha (2014), Discrete Cosine Transform based fusion of multi-focus images for visual sensor networks, Vol: 95, *Signal Processing*, pp. 161–170. <https://doi.org/10.1016/j.sigpro.2013.09.001>.
- [7] M W Jian et al (2011), Image retrieval using wavelet-based salient regions, Vol. 59, *The Imaging Science Journal*, pp. 219-231. <https://doi.org/10.1179/136821910X12867873897355>.
- [8] Qiangui Huang, Boya Hao, Sheng Chang (2016), Adaptive digital ridgelet transform and its application in image denoising, Vol. 52, *Elsevier Digital Signal Processing*, pp. 45–54. <https://doi.org/10.1016/j.dsp.2016.02.004>.
- [9] Melkamu Hunegnaw Asmare, Vijanth S. Asirvadam, Ahmad Fadzil M. Hani (2015), Image enhancement based on contourlet transform, Vol 9, *Signal, Image and Video Processing*, pp 1679–1690. <https://doi.org/10.1007/s11760-014-0626-7>.
- [10] Wei Tian et al (2015), An adaptive blind digital watermarking scheme in shearlet domain, Vol. 8, *Int. J. of Wireless and Mobile Computing*, pp. 353 – 358. <https://doi.org/10.1504/IJWMC.2015.070940>.
- [11] James M. Murphy, Jacqueline Le Moigne, David J. Harding (2016), Automatic Image Registration of Multimodal Remotely Sensed Data with Global Shearlet Features, Vol. 54, *IEEE Transactions on Geoscience and Remote Sensing*, pp. 1685 – 1704. <https://doi.org/10.1109/TGRS.2015.2487457>.
- [12] Manesh Kokare et al (2005), Cosine-Modulated Wavelet Packet based Texture Features for Content based Image Retrieval, Vol. 51, *IETE Journal of Research*, pp. 477-483. <https://doi.org/10.1080/03772063.2005.11416428>.
- [13] Yongsheng Dong et al. (2015), Texture Classification and Retrieval Using Shearlets and Linear Regression, Vol. 45, *IEEE Transactions on Cybernetics*, pp. 358 – 369. <https://doi.org/10.1109/TCYB.2014.2326059>.
- [14] Shiv Ram Dubey et al (2015), Local Wavelet Pattern: A New Feature Descriptor for Image Retrieval in Medical CT Databases, Vol. 24, *IEEE Transactions on Image Processing*, pp. 5892 – 5903.
- [15] Jiangping He, Hongwei Ji, Xin Yang (2013), Rotation Invariant Texture Descriptor Using Local Shearlet-Based Energy Histograms, Vol. 20, *IEEE Signal Processing Letters*, pp. 905 – 908.
- [16] Amani Alahmadi et al (2017), Passive detection of image forgery using DCT and local binary pattern, Vol 11, *Signal, Image and Video Processing*, pp 81–88. <https://doi.org/10.1007/s11760-016-0899-0>.
- [17] Santosh Kumar Vipparthi et al (2015), Directional local ternary patterns for multimedia image indexing and retrieval, Vol. 8, *Int. J. of Signal and Imaging Systems Engineering*, pp. 137 – 145. <https://doi.org/10.1504/IJSISE.2015.070485>.
- [18] Srinivasa Perumal Ramalingam et al (2016), Two-level dimensionality reduced local directional pattern for face recognition, Vol. 8, *Int. J. of Biometrics*, pp. 52 – 64. <https://doi.org/10.1504/IJBM.2016.077150>.
- [19] Shankar Bhausahab Nikam (2008), Local binary pattern and wavelet-based spoof fingerprint detection, Vol. 1, *Int. J. of Biometrics*, pp. 141 – 159. <https://doi.org/10.1504/IJBM.2008.020141>.
- [20] Joao B.Florindo, Odemir M.Bruno (2016), Local fractal dimension and binary patterns in texture recognition, Vol 78, *Pattern Recognition Letters*, pp. 22-27. <https://doi.org/10.1016/j.patrec.2016.03.025>.
- [21] Muhammad Hussain et al (2013), Gender recognition from face images with dyadic wavelet transform and local binary pattern, Vol. 22, *International Journal on Artificial Intelligence Tools*.
- [22] S. He, J. J. Soraghan, B. F. O'Reilly, and D. Xing (2009), Quantitative analysis of facial paralysis using local binary patterns in biomedical videos, Vol. 56, *IEEE Trans. Biomed. Eng.*, pp. 1864-1870. <https://doi.org/10.1109/TBME.2009.2017508>.
- [23] Loris Nannia, Alessandra Luminia, Sheryl Brahnam (2010), Local binary patterns variants as texture descriptors for medical image analysis Vol. 49, *Artificial Intelligence in Medicine*, pp. 117–125. <https://doi.org/10.1016/j.artmed.2010.02.006>.
- [24] A. Suruliandi, G. Murugeswari, and P. Arockia Jansi Rani (2015), Empirical Evaluation of Generic Weighted Cubicle Pattern and LBP Derivatives for Abnormality Detection in Mammogram Images, Vol. 15, *International Journal of Image and Graphics*
- [25] Wankou Yang et al. (2016), Face recognition using adaptive local ternary patterns method, Vol 213, *Neurocomputing*, pp. 183-190. <https://doi.org/10.1016/j.neucom.2015.11.134>.
- [26] Guo, L. Zhang, and D. Zhang (2010), A completed modelling of local binary pattern operator for texture classification, Vol. 19, *IEEE Trans. Image Process*, pp. 1657–1663.
- [27] S. Liao, M.W. K. Law, and A. C. S. Chung (2009), Dominant local binary patterns for texture classification, Vol. 18, *IEEE Trans. Image Process*, pp. 1107–1118. <https://doi.org/10.1109/TIP.2009.2015682>.
- [28] G. Deep et al (2017), Local quantized extrema quinary pattern: a new descriptor for biomedical image indexing and retrieval, *Computer Methods in Biomechanics and Biomedical Engineering: Imaging & Visualization*, pp 1-17. <https://doi.org/10.1080/21681163.2017.1344933>.
- [29] Timo Ahonen et al, "Rotation Invariant Image Description with Local Binary Pattern Histogram Fourier Features", SCIA '09 Proceedings, July 2009.
- [30] Maryam Nabil Al-Berry et al Salem (2016), Fusing directional wavelet local binary pattern and moments for human action recognition, Vol. 10, *IET Computer Vision*, pp. 153 – 162.
- [31] Lijian Zhou et al (2014), Face recognition based on curvelets and local binary pattern features via using local property preservation, Vol. 95, *Journal of Systems and Software*, pp. 209-216. <https://doi.org/10.1016/j.jss.2014.04.037>.
- [32] Hemprasad Y.Patil et al (2016), Expression invariant face recognition using local binary patterns and contourlet transform, Vol. 127, *International Journal for Light and Electron Optics*, pp. 2670-2678. <https://doi.org/10.1016/j.ijleo.2015.11.187>.
- [33] Jiangping He et al (2013), Rotation Invariant Texture Descriptor Using Local Shearlet-Based Energy Histograms, Vol. 20, *IEEE Signal Processing Letters*, pp. 905 – 908.
- [34] Murala, Maheshwari, Balasubramanian, "Local tetra patterns: a new feature descriptor for content-based image retrieval", *IEEE Trans Image Process*. 2012 May; 21(5):2874-86. <https://doi.org/10.1109/TIP.2012.2188809>.
- [35] Ojala, T., Pietikainen, M., Maenpaa, T. (2002), Multiresolution gray-scale and rotation invariant texture classification with local binary patterns, *IEEE Trans. Pattern Anal. Mach. Intell.* pp. 971–987. <https://doi.org/10.1109/TPAMI.2002.1017623>.
- [36] T. Ahonen, A. Hadid, and M. Pietikainen (2006), Face description with local binary patterns: Applications to face recognition, Vol. 28, *IEEE Trans. Pattern Anal. Mach. Intell.*, pp. 2037-2041. <https://doi.org/10.1109/TPAMI.2006.244>.
- [37] Corel 1K database from <http://wang.ist.psu.edu/docs/home.shtml#download>.
- [38] Corel 10K database from <https://sites.google.com/site/dctresearch/Home/content-based-image-retrieval>.
- [39] Brodatz database http://multibandtexture.recherche.usherbrooke.ca/original_brodatz.html.
- [40] Shiv Ram Dubey et al (2015), Boosting local binary pattern with bag-of-filters for content based image retrieval, *IEEE UP Section Conference on Electrical Computer and Electronics (UPCON)*. <https://doi.org/10.1109/UPCON.2015.7456703>.
- [41] Subrahmanyam Murala, Maheshwari, Balasubramanian (2012), Directional Binary Wavelet Patterns for Biomedical Image Indexing and Retrieval, Vol. 36, *Journal of Medical Systems*, pp. 2865-2879. <https://doi.org/10.1007/s10916-011-9764-4>.